

Proximity gettering process for 300-mm silicon wafers

Gon-Sub Lee* and Jea-Gun Park

Nano-SOI Process Laboratory, Hanyang University, 17 Haengdang-Dong, Seoungdong-Gu, Seoul 133-791, Korea

The development of an effective proximity gettering process is a key material engineering consideration for advanced semiconductor devices fabricated on 300-mm silicon wafers. Effective intrinsic gettering can be achieved by applying rapid thermal annealing (RTA) in a gas mixture of ammonia and argon at around 1150°C, which produces the desired "M"-shaped depth profile for the oxygen precipitates in the silicon bulk. The depth of the denuded zone is adjustable, and the peak density of the oxygen precipitates is above $1 \times 10^{10} \text{ cm}^{-3}$. The peak density strongly depends on the RTA temperature and the wafer's initial interstitial oxygen concentration, so a higher temperature and higher initial interstitial oxygen concentration in the wafer lead to a higher density of oxygen precipitates. The "M"-shaped profile originates from the vacancy profile produced after cooling down from the RTA process. Utilizing the ammonia/argon gas mixture reduces the RTA temperature so as to obtain a higher density of oxygen precipitates and reduces slip in the wafer, as compared to performing RTA under a gas mixture of nitrogen and argon.

Key words: RTA, oxygen precipitates, vacancy, proximity gettering, 300-mm silicon wafer.

Introduction

In ultra large-scale integration device fabrication, heavy metal contamination is a critical issue, as the allowable level of metallic contamination decreases as the design rule becomes tighter. Specifically, for devices with a design rule of less than 0.18 mm, the contamination should be kept below $1 \times 10^{10} \text{ cm}^{-2}$ on the wafer surface and in the bulk [1]. In addition, as device processes advance, the accumulated diffusion length becomes much longer than the typical wafer thickness.

For several years, the study of gettering by the elimination of metallic contamination during device processes, has been a major field of materials engineering research for device and wafer fabrication. Several traditional methods have been utilized to increase the gettering capability of wafers, including high-low-high heat treatment [2-10] for intrinsic gettering, and poly-Si deposition [11-13] and POCl_3 diffusion [14, 15] on the wafer backside for extrinsic gettering. The conventional intrinsic gettering processes have several disadvantages, such as an instability in controlling the defect-free region (denuded zone), cross-metallic contamination, and high production costs due to the long duration of the heat treatment. The traditional extrinsic gettering methods also have disadvantages, such as the generation of small particles during device processes like cleaning, and a relatively weak gettering capability.

In this study, to provide a powerful intrinsic gettering capability, we propose a rapid thermal annealing (RTA) process [16, 17] with no disadvantages, such as slip in 300-mm wafers. We also discuss the effect of the gas mixture used in high-temperature RTA on the intrinsic gettering capability.

Experiment

The samples used in this experiment were p-type, 10- Ω -cm, (100) orientation, 300-mm polished silicon wafers with an initial interstitial oxygen concentration of 10.3 ppma (ASTM F-121-81). A rapid thermal annealing (RTA) process (RTP1200) was applied over a temperature range from 1100 to 1200 °C in 10 °C steps under an ammonia and argon gas mixture. For comparison, a separate RTA process was performed at 1150, 1175, 1200, and 1250 °C under a nitrogen and argon gas mixture. The wafers were subjected to heat treatment at 800 °C, for 4 hours, followed by 16 hours at 1000 °C, in a nitrogen ambient in order to observe the oxygen-precipitate density and the depth profile through an optical microscope, after performing Secco etching on the cleaved wafers for 3 minutes. To observe slip formation, the wafers were also examined by x-ray topography. To investigate the mechanism accounting for the observed depth profiles and the formation of oxygen precipitates, the vacancy concentrations and profiles of the wafers were measured by deep-level transient spectroscopy (DLTS) after platinum coating and diffusion at 760 °C for 1 hour.

*Corresponding author:
Tel : +82-2-2290-0234
Fax : +82-2-2296-1179
E-mail: gslee@hanyang.ac.kr, parkjg@hanyang.ac.kr

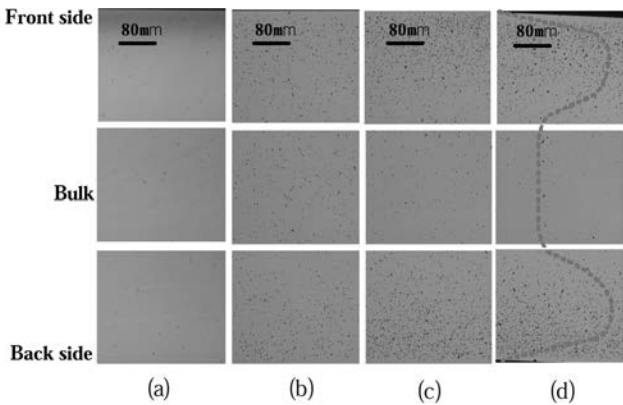


Fig. 1. Cross-sectional microscope images of the oxygen precipitate depth profiles of wafers subjected RTA under an ammonia and argon gas mixture at (a) 1100 °C, (b) 1150 °C, (c) 1170 °C, and (d) 1200 °C.

Experimental Results and Discussion

The formation of oxygen precipitates depends on the annealing temperature, annealing time, and gas ambient [5]. Figure 1 shows cross-sectional microscope images of the oxygen precipitate depth profiles of wafers subjected to RTA at (a) 1100, (b) 1150, (c) 1170, and (d) 1200 °C for 10 seconds under an ammonia and argon gas mixture. The oxygen-precipitate density increased with increasing annealing temperature. At 1150 °C and above, the density exhibited the characteristic “M”-shaped profile. This means that on each side of the wafer, after a denuded zone of about 10 μm, the density of oxygen precipitates increased and then decreased to reach a denuded zone at a depth of 200 μm in the silicon bulk. Figures 1(b), (c), and (d) clearly shows this “M”-shaped oxygen precipitate profile.

Figure 2 shows the oxygen-precipitate density as a function of temperature for 10 seconds of RTA under both the NH₃/Ar and N₂/Ar gas mixture. The density increased with increasing annealing temperature under

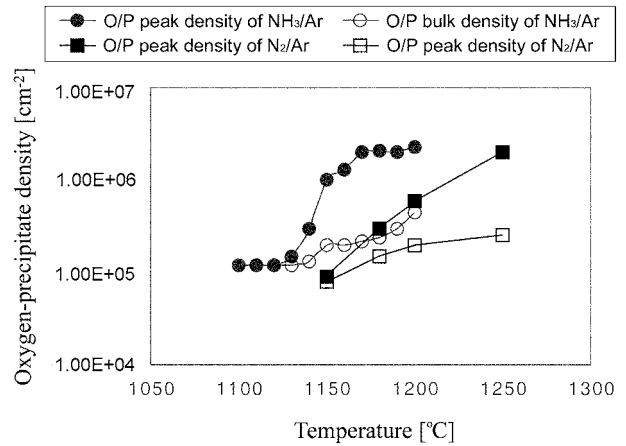


Fig. 2. Oxygen-precipitate density with respect to RTA temperature under NH₃/Ar and N₂/Ar gas mixtures.

both gas mixtures. At the same annealing temperature, however, the density was higher with the NH₃/Ar mixture than with the N₂/Ar mixture. For example, the density at 1150 °C in the NH₃/Ar case was $1 \times 10^6 \text{ cm}^{-2}$, which is almost the same as the density at 1250 °C in the N₂/Ar case. In both cases, the peak oxygen-precipitate density and bulk oxygen-precipitate density were $1\sim 2 \times 10^6 \text{ cm}^{-2}$ and $2 \times 10^5 \text{ cm}^{-2}$. This demonstrates a significant advantage of using a gas mixture of ammonia and argon, in that it minimize the risk of slip formation due to the reduced temperature required for effective RTA.

Figure 3 shows the oxygen-precipitate density as a function of annealing time for RTA under the N₂/Ar gas mixture at 1250 °C and the NH₃/Ar gas mixture at 1150 °C. In both cases, as the RTA time increased, the oxygen-precipitate density also increased. This shows that the 1150 °C NH₃/Ar process coincided well with the 1250 °C N₂/Ar process.

Figure 4 show the relationship between the oxygen-precipitate density and the initial interstitial oxygen concentration of the wafers for 10 seconds of RTA

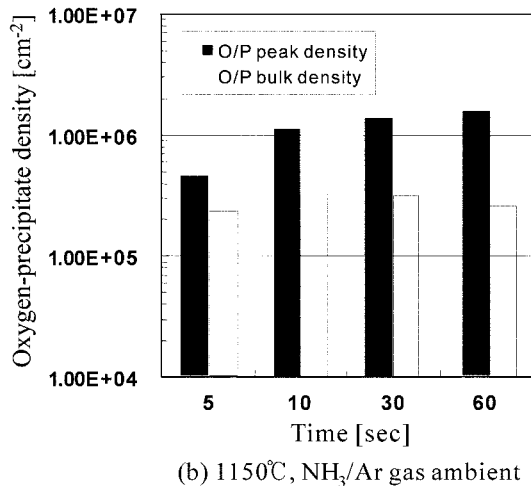
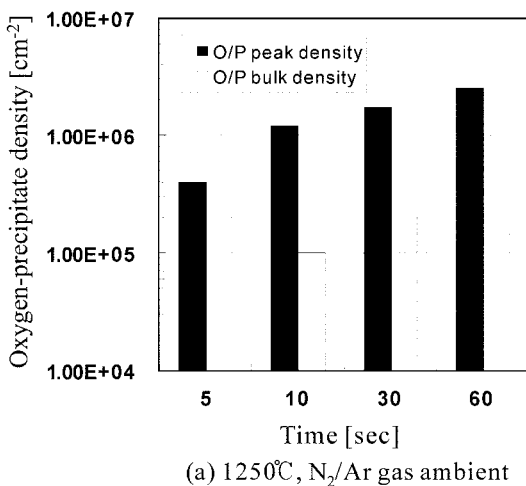


Fig. 3. Oxygen-precipitate density with respect to RTA time under (a) a N₂/Ar gas mixture at 1250 °C and (b) NH₃/Ar gas mixture at 1150 °C.

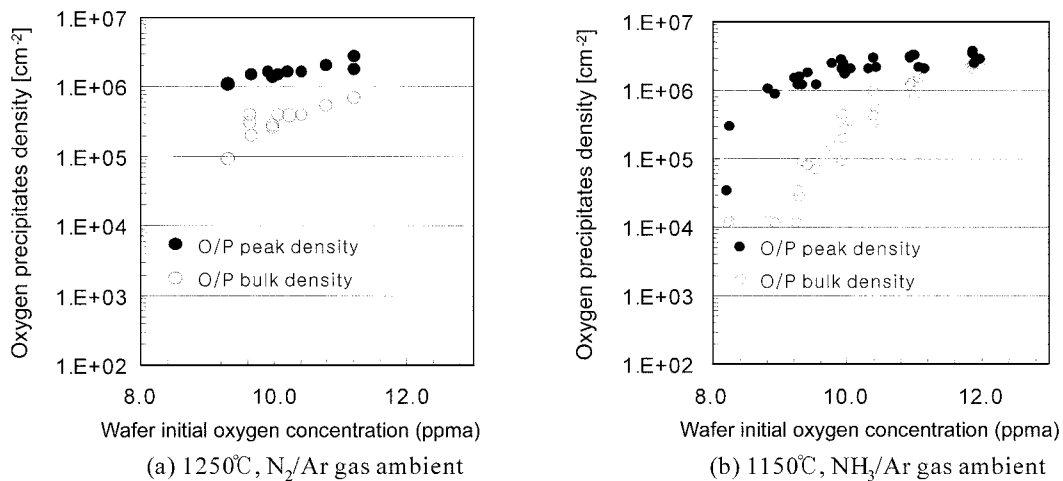


Fig. 4. Oxygen-precipitate density as a function of the wafer's initial interstitial oxygen concentration under (a) the N₂/Ar gas mixture at 1250 °C and (b) the NH₃/Ar gas mixture at 1150 °C.

under (a) the N₂/Ar gas mixture at 1250 °C and (b) the NH₃/Ar gas mixture at 1150 °C. In both cases, the oxygen-precipitate density increased with the initial interstitial oxygen concentration. Likewise, in both cases, the difference between the peak and bulk oxygen-precipitate densities decreased as the initial interstitial oxygen concentration increased. This is because a higher initial interstitial oxygen concentration produced a greater density of oxygen precipitates in the bulk silicon after the two-step heat-treatment (i.e., 4 hours at 800 °C, followed by 16 hours at 1000 °C used to enhance the formation of the precipitates. Therefore, to obtain a high density of oxygen precipitates with an “M”-shaped profile, it is necessary to use wafers with an optimum initial interstitial oxygen concentration.

Figure 5 illustrates the relationship between the pin mark size induced by a general RTA wafer-handling system and the RTA temperature. Even at the same temperature, the NH₃/Ar process resulted in a smaller pin mark than did the N₂/Ar process. As noted in reference to Figs. 2, 3, and 4, the NH₃/Ar process at 1150 °C corresponds to the N₂/Ar process at 1250 in

terms of the oxygen-precipitate density. The capability of the NH₃/Ar process to minimize the risk of pin mark formation by a general pin-type RTA wafer-handling system is thus a significant advantage in favor of this process.

Figure 6 shows an actual example of a slip-free 300-mm wafer subjected to RTA in a NH₃/Ar gas mixture by using an edge-ring type wafer-handling system. To facilitate an accelerated test, the RTA temperature was set to 1200 °C, which is higher than the temperature required for generating sufficient oxygen precipitation. X-ray topography demonstrated that wafer slip did not appear on the wafer surface or in the bulk. This indicates that using an edge-ring type wafer-handling system during RTA reduced the degree of slip generation as compared to using a pin-type system, because the amount of slip is reduced by ensuring a larger contact area.

To understand the mechanism of oxygen precipitation, the vacancy concentration was measured by DLTS after platinum coating and diffusion at 760 °C for 1 hour. Figure 7 illustrates the relationship between the oxygen-

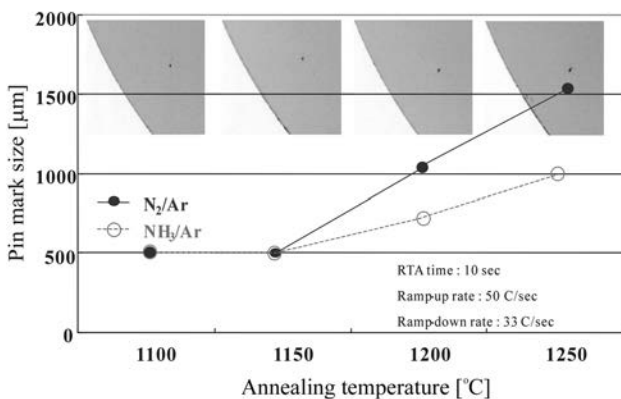


Fig. 5. Relationship between the pin mark size and the RTA temperature for the N₂/Ar and NH₃/Ar gas mixtures.

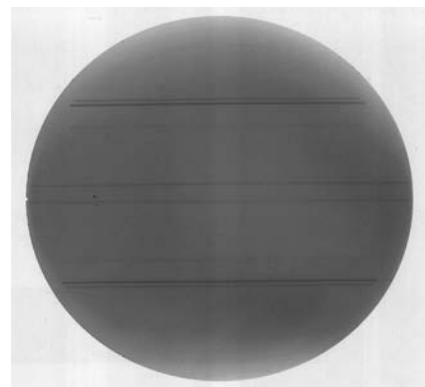


Fig. 6. X-ray topography image of a slip-free 300-mm silicon wafer.

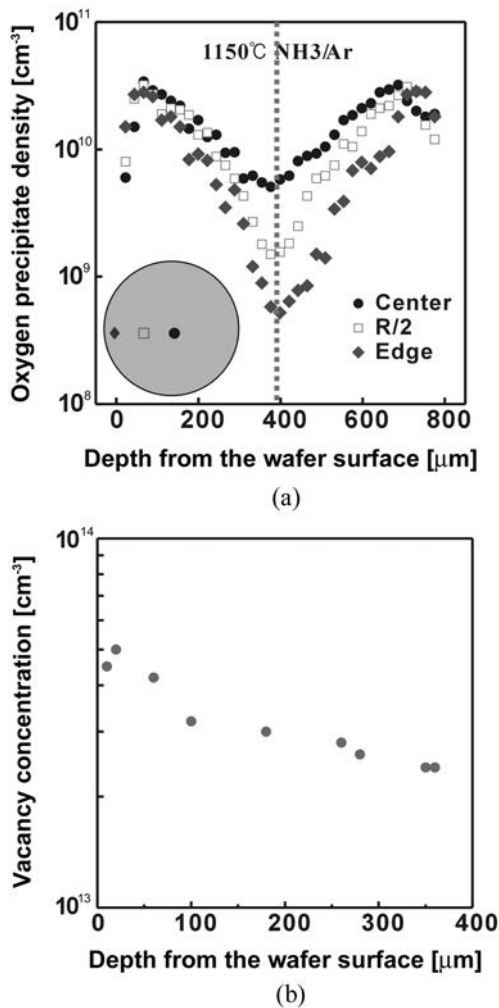
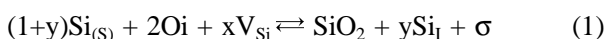


Fig. 7. (a) Depth profile of the oxygen-precipitate density after heat treatment for 4 hours at 800 °C, followed by 16 hours at 1000 °C. (b) Depth profile of the vacancy concentration after platinum coating and diffusion at 760 °C for 1 hour.

precipitate density profile and the vacancy concentration profile. Figure 7(a) shows the oxygen-precipitate density as a function of the wafer depth profile for the NH₃/Ar process at 1150 °C. This density exhibited the typical “M”-shaped profile at the wafer’s center, at the half the radius from the center (denoted as “R/2” in the figure), and at the wafer’s edge. Figure 7(b) shows the vacancy depth profile measured by DLTS under the conditions noted above. The vacancy profile exhibited a higher density near the wafer’s surface and then decreased with increasing depth in the bulk. The vacancy profile thus coincided well with the depth profile of the oxygen-precipitate density. As a result, we can speculate that the oxygen precipitation mechanism is closely related to the vacancy behavior, as indicated by the following chemical reaction.



This reaction suggests that the oxygen-precipitate density increases with the RTA temperature, the RTA

time, and the initial interstitial oxygen concentration of the wafers, under both the NH₃/Ar and N₂/Ar gas mixtures, which corresponds to the results of our experiments. The density of oxygen precipitates for the NH₃/Ar process, however, is expected to be higher than that for the N₂/Ar process at the same temperature, since the injection rate of point defects, such as silicon vacancies, is higher under the NH₃/Ar gas ambient. This behavior also corresponds to the experimental results.

Conclusions

Rapid thermal annealing (RTA) produces a supersaturation of vacancies in silicon via fast cooling, and it injects point defects, such as vacancies, when it is performed under a NH₃/Ar or N₂/Ar gas mixture. The resulting density of oxygen precipitates increases with the RTA temperature, the RTA time, and the initial interstitial oxygen concentration of the wafers, under both gas mixtures. The typical “M”-shaped depth profile for oxygen precipitates, which is desirable for proximity gettering in ULSI device fabrication, was obtained without slip formation on a 300-mm silicon wafer after RTA at 1150 °C for 10 seconds in a NH₃/Ar gas mixture.

Acknowledgement

This work was supported by the Korea Ministry of Science and Technology through the National Research Laboratory (NRL) program. We thank Sumitomo Mitsubishi Silicon Corp. and Kornic System for helping us with our experiments.

References

1. International Tech. Roadmap Semiconductor, 99, Starting Materials.
2. T.Y. Tan, E.E. Gardner, and W.K. Tice, *Appl. Phys. Lett.* 30 (1977) 175-176.
3. S. Kishino, S. Isomae, M. Tamura, and M. Maki, *Appl. Phys. Lett.* 32 (1978) 1-3.
4. K.H. Yang, H.F. Kappert, and G.H. Schwuttke, *Phys. Stat. Sol.* 50 (1978) 221.
5. H. Tsuya, K. Tanno, and F. Shimura, *Appl. Phys. Lett.* 36 (1980) 658-660.
6. H.R. Huff, H.F. Schaake, J.T. Robinson, S.C. Baber, and D. Wong, *J. Electrochem. Soc. Solid-State Science and Technology*, July, 130 (1983) 1551-1555.
7. S. Kishino, T. Aoshima, A. Yoshinaka, H. Shimizu, and M. Ono, *Jpn. J. Appl. Phys.* 23 (1984) L9-L11.
8. T.A. Baginski and J.R. Monkowski, *J. Electrochem. Soc.* April, 133 (1986) 762-168.
9. M.B. Shabani, S. Okuuchi, T. Yoshimi, T. Shingyoji, and F.G. Kirschy, *Electrochem. Soc. PV98-13* (1998) 313-327.
10. S. Koveshnikov, O. Kononchuk, K. Beaman, Rozgonyi, and F. Gonzalez, *Electrochem. Soc. PV98-13* (1998) 341-354.
11. L. Baldi, G. Cerofolini, and G. Ferla, *J. Electrochem. Soc.* (1980) 164.
12. R. Falster, Ph.D Thesis, Stanford University (1983).

13. R.W. Shaw, H.K. Korb, and C.P. Reed, *Electrochem. Soc.* (1985) 353-364.
14. T.E. Seidel and R.L. Meek, 305, Plenum Press, New York (1973).
15. R.L. Meek, T.E. Seidel, and A.G. Cullis, *J. Electrochem. Soc., Solid-State Science and Technology*, June (1975) 786-796.
16. R. Falster, D. Gambaro, M. Olmo, M. Cornara, and H. Korb. *ECS PV98-13* (1998) 135-146.
17. H. Takeno, K. Aihara, Y. Hayamizu, and T. Masui, *Electrochem. Soc. PV99-1* (1999) 150-161.